Electronic Supplementary Material (ESI) for Chemical Communications.
This journal is © The Royal Society of Chemistry 2016

Supplementary Information for:

High-Throughput Synthesis and Characterization of Nanocrystalline Porphyrinic Zirconium Metal-Organic Frameworks

Margaret L. Kelty,[1†] William Morris,[1†] Audrey T. Gallagher,[1] John S. Anderson,[1] Keith A. Brown,[1,2] Chad A. Mirkin,[1-3]* T. David Harris[1]*

1. Department of Chemistry, Northwestern University, 2145 Sheridan Road, Evanston, IL 60208
2. International Institute for Nanotechnology, Northwestern University, 2145 Sheridan Road, Evanston, IL 60208
3. Department of Materials Science and Engineering, Northwestern University, 2220 Campus Dive, Evanston, IL 60208

[†] These authors contributed equally to this work

Email: chadnano@northwestern.edu
dharris@northwestern.edu

Chem. Commun.

Table of Contents

Experimental Section

General Considerations. All chemicals were purchased from commercial vendors and used without further purification or synthesized from literature procedures.[1]

High-Throughput Synthesis. Reported syntheses of H_6TCPP zirconium compounds are carried out in dimethylformamide (DMF) or diethylformamide (DEF) and proceed through self-assembly reactions involving the following components: tetracarboxyphenyl porphyrin (H_6TCPP) to serve as the organic linker; a zirconium source to provide the metal cluster node, and a monotopic carboxylic acid to modulate nucleation of the crystallites. [2-5] High-throughput reaction conditions were selected through the systematic variation of stoichiometry, temperature, reaction time, and solvent. Metal and modulator reactants were also varied, with $ZrCl_4$ or $ZrOCl_2 \cdot 8H_2O$ serving as the source of zirconium, and acetic acid, benzoic acid, formic acid, or dichloroacetic acid serving as the acid source.

A Gilson GX-271 liquid handler was programmed to dispense aliquots of liquid reagents (dichloroacetic acid, acetic acid, and formic acid) and stock solutions of solid reagents (tetracarboxyphenyl porphyrin, zirconium source, and benzoic acid) dissolved in DMF or DEF into 1.8 mL borosilicate vials arranged in a 96-well holder. The automated programs were designed such that, in most cases, neighboring reactions were identical except for one variable. The 96 reactions from each automated run were then heated at 90, 120, or 130 °C for 18 or 72 hours. In total, twelve different automated runs were carried out, corresponding to 1027 unique sets of reaction conditions and 1036 total reactions.

Preparative-Scale Synthesis. Crystalline and pure-phase reaction conditions discovered through high-throughput synthesis were employed on with a scale-up of 4 (PCN-223), 5 (MOF-525), or 15-fold (MOF-545), using either 11 mL or 22 mL borosilicate vials with Teflon-lined caps. Upon scale-up of each set of conditions, acid volume was varied incrementally across a series of 5-12 reactions. For MOF-525, the volume of acetic acid was varied from 0.20 to 0.40 mL. For MOF-545, the volume of dichloroacetic acid was varied from 0.25 to 0.60 mL. For PCN-223, the volume of acetic acid was varied from 0.15 to 0.70 mL. Procedures corresponding to successful syntheses for each compound and its corresponding size scale are described below.

Synchrotron Powder X-Ray Diffraction (PXRD) Characterization. Reaction products from high-throughput syntheses were transferred directly from reaction mixtures, without further purification or solvent exchange, to thin-walled quartz capillary tubes with a 1.5 mm outer diameter. The products were allowed to settle to the bottom of the capillaries and excess solution was removed by a syringe. PXRD data were collected at the Advanced Photon Source of Argonne National Laboratory with the DuPont-Northwestern-Dow Collaborative Access team (DND-CAT) at Beamline 5-ID-D. Powder X-ray diffraction patterns were collected at a wavelength of 1.239 Å with exposure times of one second. The large background observed in the powder patterns can be attributed to suspension of the samples in solution. For samples collected at Argonne National Lab, a break in the powder pattern between 2θ values of 5.3 and 5.4 is observed as a result of the instrument switching from a medium angle to a wide angle detector.

Pattern Matching. Powder X-ray patterns collected at Argonne National Laboratory were rigorously analyzed using a custom-made pattern-matching MATLAB program (available for download in the ESI). Medium and high angle one-dimensional pattern averages were entered into the program, and the experimental peaks were compared to simulated patterns obtained from published single-crystal X-ray data. Simulated patterns were generated for MOF-525,[2] MOF-545,[Error! Bookmark not defined.] PCN-223,[3] PCN-224,[4] and PCN-225.[5] The program identifies all peaks in the experimental spectra, evaluates their center, magnitude and width using non-linear least squares fitting to a Lorentzian line shape, and compares the experimental peaks to a library of known peaks. The output of this program is a matrix in which each experimental pattern is compared to simulated patterns generated for the five known TCPP-based Zr_6 MOF morphologies. The diffraction peaks in the experimental data are then compared to the simulated patterns and the number of peaks that match and do not match is recorded. Based on the number of peaks in each category, the program assigns the experimental pattern to a known structure or indicates the lack of any match. The program also graphs each experimental pattern (see Figure S2 and S3): red circles are placed on every peak detected by the program and blue circles highlight the peaks considered in pattern matching. Colored bars are placed along to bottom to indicate where peaks are expected for each simulated pattern.

MATLAB pattern matching analysis. Data from the matrix generated by the MATLAB program were exported to an excel spreadsheet and reactant concentrations were added to the corresponding PXRD results. In total, 381 patterns were collected and exported into the spreadsheet. If multiple patterns were collected for a single reaction, the graphs generated by the MATLAB program were compared to the matrix assignment. The assignment which most accurately resembled the graphed pattern was chosen. After duplicate results were removed, 254 patterns remained for examination. Although the MATLAB program will assign patterns with no peaks as "No Match", manual examination of the results revealed that no peaks were recorded for 85 of the patterns. The data were then compiled into tables based on reaction conditions (see Tables S1-S5).

Powder X-Ray Diffraction Analysis of Preparative-Scale Syntheses. Preparative-scale syntheses yielding MOF-525, MOF-545, and PCN-223 were purified by centrifugation (15000 rpm, 5 min) followed by solvent exchange with DMF (3 × 1 mL) and then acetone (3 × 1 mL). The products were dried under reduced pressure at 150 °C for 12 hours, and the solid material was then transferred to a thin-walled quartz capillary tube with a 1.5 mm outer diameter. Powder X-ray diffraction patterns were collected using a Rigaku model ATXG diffractometer equipped with CuKα radiation. The tube voltage and current were 50 kV and 240 mA, respectively.

Electron Microscopy. High-throughput and preparative-scale syntheses yielding MOF-525, MOF-545, and PCN-223 were purified by centrifugation (15000 rpm, 5 min) followed by solvent exchange with DMF (3 × 1 mL) and then acetone (3 × 1 mL). The samples were suspended in acetone without drying to prevent aggregation and drop cast onto a 400-mesh copper grid. Images were collected on a Hitachi HD-2300 Dual EDS Cryo S/TEM in either scanning electron or transmission electron mode with an accelerating voltage of 200 kV. The dimensions of 55 to 72 crystals were measured to determine the average size and standard deviation for each morphology.

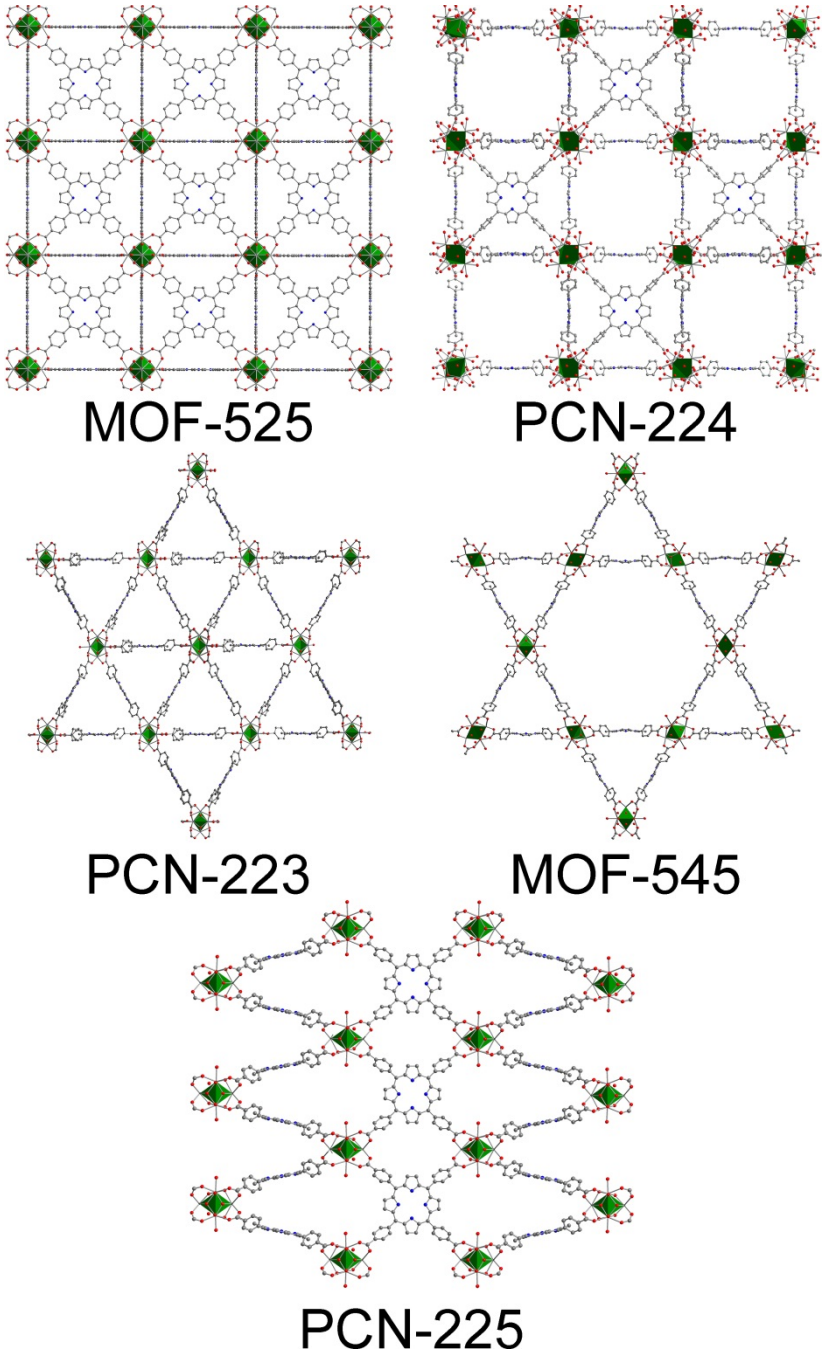

Figure S1 | Crystal structures of porphyrinic zirconium MOFs featuring tetracarboxyphenyl porphyrin (H_6TCPP) linkers and Zr_6 nodes. Green octahedra represent zirconium atoms, while red, blue, and grey spheres represent oxygen, nitrogen, and carbon atoms, respectively; hydrogen atoms are omitted for clarity. MOF-525[Error! Bookmark not defined.] and PCN-223[Error! Bookmark not defined.] feature 12-connected Zr_6 clusters, MOF-545[Error! Bookmark not defined.] and PCN-225[Error! Bookmark not defined.] feature 8-connected Zr_6 clusters and PCN-224[Error! Bookmark not defined.] features 6-connected Zr_6 clusters.

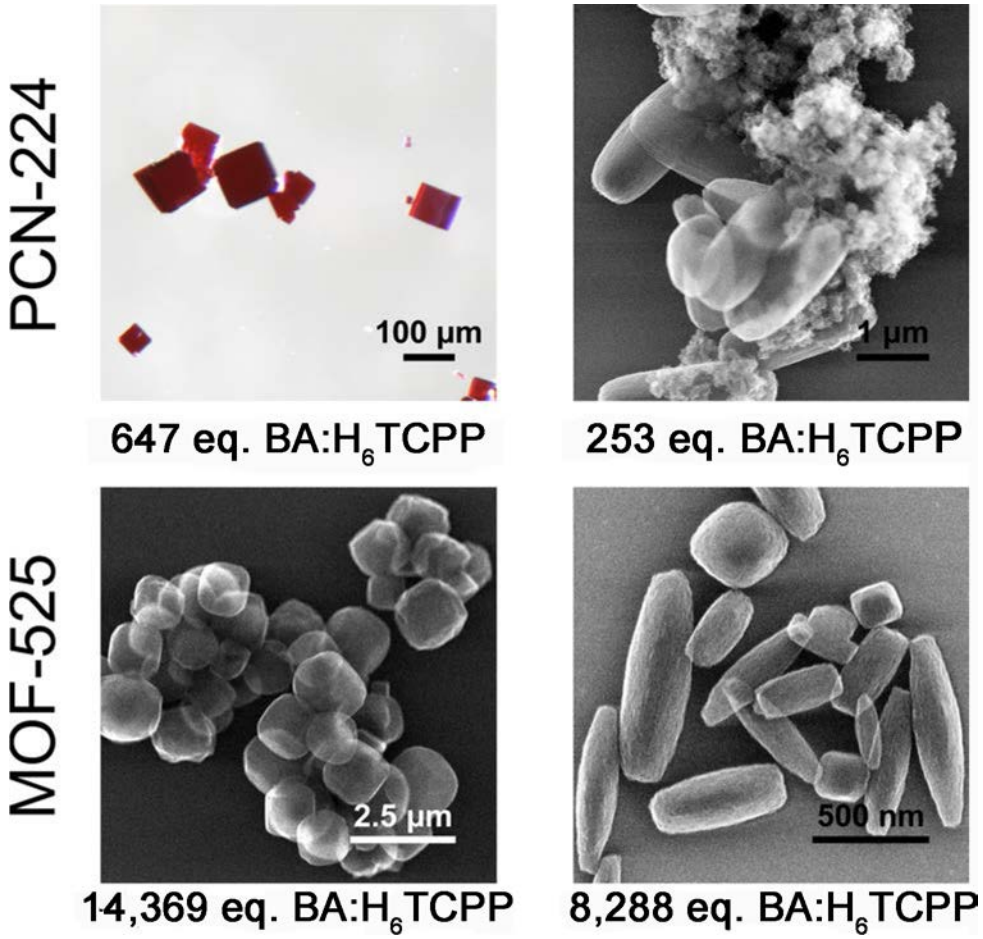

Figure S2 | Previous reports have shown that increasing the concentration of additional monotopic carboxylic acid modulators can aid in the formation of macrocrystals of the zirconium MOF UiO-66 and are directly associated with defect-rich structures.[6-9] Accordingly, our initial attempt to synthesize nanocrystals of porphyrinic zirconium MOFs involved simply decreasing the acid concentration relative to the published syntheses of macroscale analogues. However, this strategy resulted exclusively in mixed-phase and amorphous products and further underscored to us the need for a high-throughput method to rapidly screen a wide range of reaction conditions. Shown above are optical and EM images of reaction products prepared from published syntheses for PCN-224[4] and MOF-525[Error! Bookmark not defined.] (left column) and show the incorporation of multiple phases and amorphous products upon decreasing benzoic acid (BA) equivalents (right column). Differently shaped particles reflect different structures.

Section S1 | High-throughput nanocrystalline MOF syntheses

Run 1, reaction 8: nanoscale MOF-545. Stock solutions were prepared in DMF for tetrakis(4-carboxyphenyl)porphyrin (0.87 g/L, 0.0011 M) and zirconyl chloride octahydrate (5.0 g/L, 0.016 M). The porphyrin solution (500 μL, 0.00043 g, 0.00055 mmol) was dispensed into a 0.5 dram pyrex vial. The zirconium solution (500 μL, 0.0025 g, 0.0078 mmol) was then added, followed by dichloroacetic acid (30 μL, 0.36 mmol) and additional DMF (70 μL) to give a total volume of 1,100 μL. The vial was heated at 130 °C for 18 hours.

Run 7, reaction 83: nanoscale MOF-525. Stock solutions were prepared in DMF for tetrakis(4-carboxyphenyl)porphyrin (9.8 g/L, 0.012 M) and zirconyl chloride octahydrate (5.2 g/L, 0.016 M). The porphyrin solution (200 μL, 0.0020 g, 0.0025 mmol) was dispensed into a 0.5 dram pyrex vial. The zirconium solution (200 μL, 0.0010 g, 0.0032 mmol) was then added, followed by acetic acid (65 μL, 0.0011 mmol) and additional DMF (200 μL) to give a total volume of 665 μL. The vial was heated at 90 °C for 18 hours.

Run 12, reaction 15: nanoscale PCN-223. Stock solutions were prepared in DMF for tetrakis(4-carboxyphenyl)porphyrin (6.10 g/L, 0.0077 M) and zirconyl chloride octahydrate (4.30 g/L, 0.013 M). The porphyrin solution (400 μL, 0.0025 g, 0.0031 mmol) was dispensed into a 0.5 dram pyrex vial. The zirconium solution (300 μL, 0.0013 g, 0.0040 mmol) was then added, followed by acetic acid (160 μL, 0.0028 mmol) and additional DMF (50 μL) to give a total volume of 910 μL. The vial was heated at 90 °C for 18 hours.

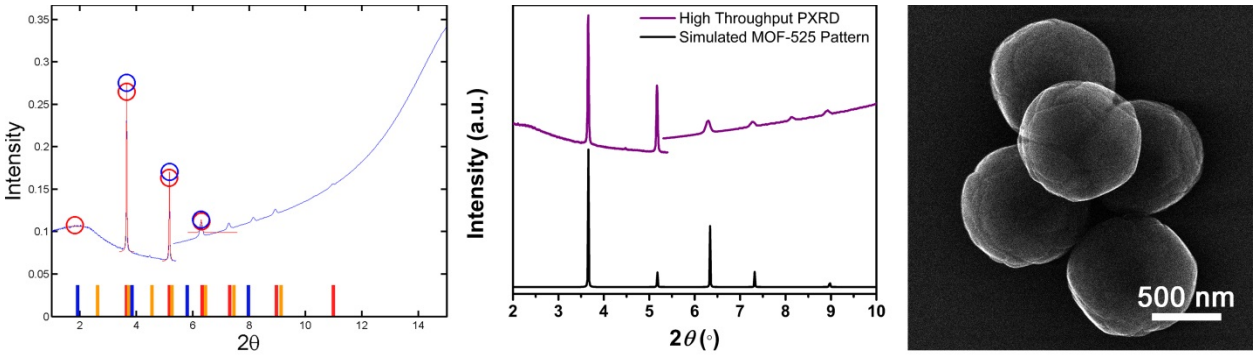

Figure S3 | Data collected for the high-throughput reaction that resulted in the synthesis of nanocrystalline MOF-525. The graph on the left was generated by the peak matching MATLAB program. Red circles indicate detected peaks and blue circles indicate peaks that were compared to simulated patterns. The middle graph shows the same pattern from 2 to 10°. The middle graph shows the same pattern from 2 to 10°. For samples collected at Argonne National Lab, a break in the powder pattern between 2θ values of 5.3 and 5.4 is observed as a result of the instrument switching from a medium angle to a wide angle detector mode. The TEM image on the right shows the high-throughput product. Due to particle aggregation an exact size could not be measured. An approximate size was determined from the measurement of a few crystals.

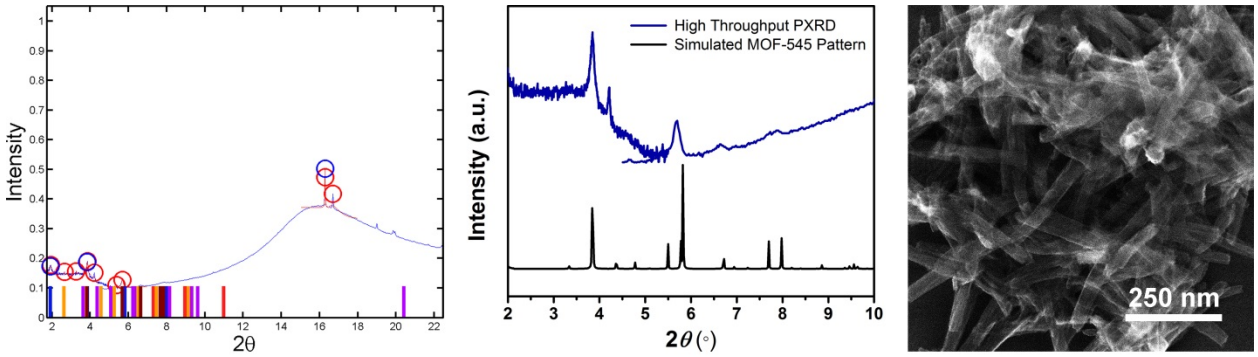

Figure S4 | Data collected for the high-throughput reaction that resulted in the synthesis of nanocrystalline MOF-545. The graph on the left was generated by the peak matching MATLAB program. Red circles indicate detected peaks and blue circles indicate peaks that were compared to simulated patterns. The middle graph shows the same pattern from 2 to 10°. The middle graph shows the same pattern from 2 to 10°. For samples collected at Argonne National Lab, a break in the powder pattern between 2θ values of 5.3 and 5.4 is observed as a result of the instrument switching from a medium angle to a wide angle detector mode. The TEM image on the right shows the high-throughput product. Due to particle aggregation an exact size could not be measured. An approximate size was determined from the measurement of a few crystals.

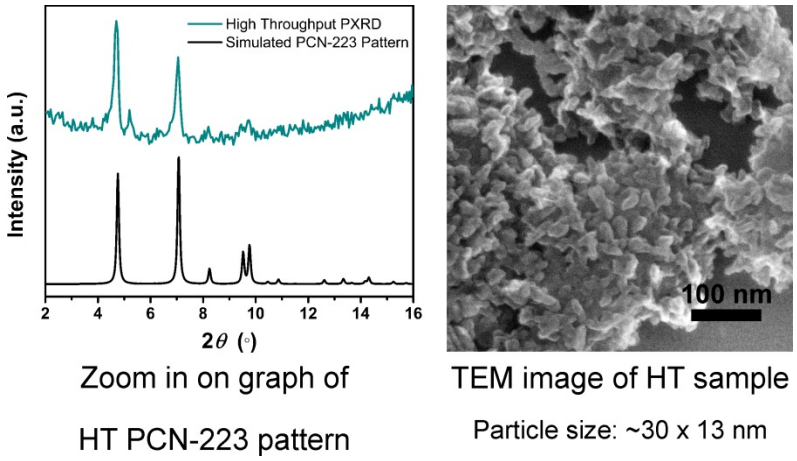

Figure S5 | Data collected for the high-throughput reaction that resulted in the synthesis of nanocrystalline PCN-223. The powder pattern was collected using the Rigaku ATXG diffractometer instead of at Argonne National Laboratory. On the right a TEM image of the high-throughput product is shown. Due to particle aggregation an exact size could not be measured. An approximate size was determined from the measurement of a few crystals.

Table S1 | Summary of high-throughput reactions

DEF - 30 rxn		
120 °C - 30 rxn		
$ZrCl_4$ - 30 rxn		
Acetic - 11 rxn	Benzoic - 11 rxn	Formic - 8 rxn

DMF - 224 rxn			
90 °C - 120 rxn			
$ZrOCl_2 \cdot 8H_2O$ - 99 rxn			$ZrCl_4$ - 21 rxn
Acetic - 78 rxn	Benzoic - 2 rxn	Formic - 19 rxn	Benzoic- 21 rxn

DMF - 224 rxn					
130 °C - 104 rxn					
$ZrOCl_2 \cdot 8H_2O$ - 30 rxn			$ZrCl_4$ - 74 rxn		
Acetic - 28 rxn	Formic - 26 rxn	Dichloroacetic - 20 rxn	Acetic - 8 rxn	Benzoic - 11 rxn	Formic - 11 rxn

The first row in each table indicates the number of reactions prepared in that solvent. The second row indicates the number of reactions carried out in that solvent at a specific temperature. The third row indicates the number of reactions with a specific zirconium source, and the fourth row indicates the carboxylic acid modulator used.

Table S2 | High-throughput MATLAB pattern matching results

254 reactions characterized by PXRD		
Assignment	# Reactions	Percent
No Peaks	85	33%
No Match	77	30%
MOF-525	42	17%
PCN-223	26	10%
MOF-545	16	6%
PCN-225	5	2%
PCN-224	3	1%

Table S3 | Temperature and solvent dependent MATLAB pattern matching results

120 reactions at 90 °C (DMF)		
Assignment	# Reactions	Percent
No Match	42	35%
No Peaks	41	34%
MOF-525	30	25%
MOF-545	3	2.5 %
PCN-224	3	2.5 %
PCN-223	1	1%

30 reactions at 120 °C (DEF)		
Assignment	# Reactions	Percent
No Peaks	12	40%
PCN-223	9	20%
No Match	4	13%
MOF-545	3	10%
PCN-225	2	7%

104 reactions at 130 °C (DMF)		
Assignment	# Reactions	Percent
No Peaks	32	31%
No Match	31	30%
PCN-223	16	15%
MOF-525	12	12%
MOF-545	10	10%
PCN-225	3	3%

Table S4 | Acid dependent MATLAB pattern matching results

128 reactions with acetic acid – p*K*a = 4.76		
Assignment	# Reactions	Percent
No Peaks	38	30%
No Match	34	27%
MOF-525	32	25%
PCN-223	14	11%
MOF-545	4	3%
PCN-224	3	2%
PCN-225	3	2%

45 reactions with benzoic acid – p*K*a = 4.2		
Assignment	# Reactions	Percent
No Peaks	18	40%
No Match	7	16%
MOF-525	7	16%
PCN-223	7	16%
MOF-545	4	9%
PCN-225	2	4%

61 reactions with formic acid – p*K*a = 3.77		
Assignment	# Reactions	Percent
No Match	32	52%
No Peaks	20	33%
MOF-525	3	5%
MOF-545	3	5%
PCN-223	3	5%

20 reactions with dichloroacetic acid – pK_a= 1.29		
Assignment	# Reactions	Percent
No Peaks	9	45%
MOF-545	5	25%
No Match	4	20%
PCN-223	2	10%

Table S5 | Zirconium dependent MATLAB pattern matching results

173 reactions with $ZrOCl_2 \cdot 8H_2O$		
Assignment	# Reactions	Percent
No Match	59	34%
No Peaks	52	30%
MOF-525	37	21%
PCN-223	12	7%
MOF-545	10	6%
PCN-224	3	2%

48 reactions with $ZrCl_4$		
Assignment	# Reactions	Percent
No Peaks	33	41%
No Match	18	22%
PCN-223	14	17%
MOF-545	6	7%
MOF-525	5	6%
PCN-225	5	6%

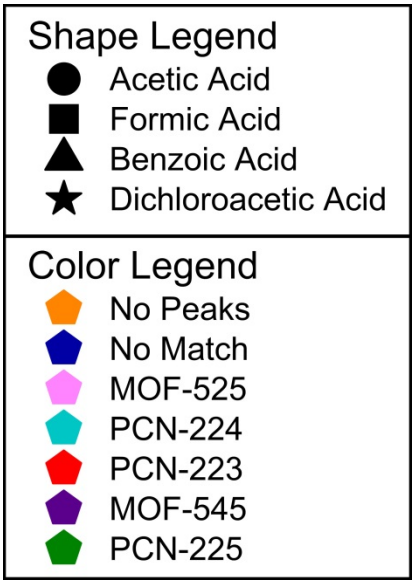

Figure S6 | Shape and color legend for data points in Figures S7-S11.

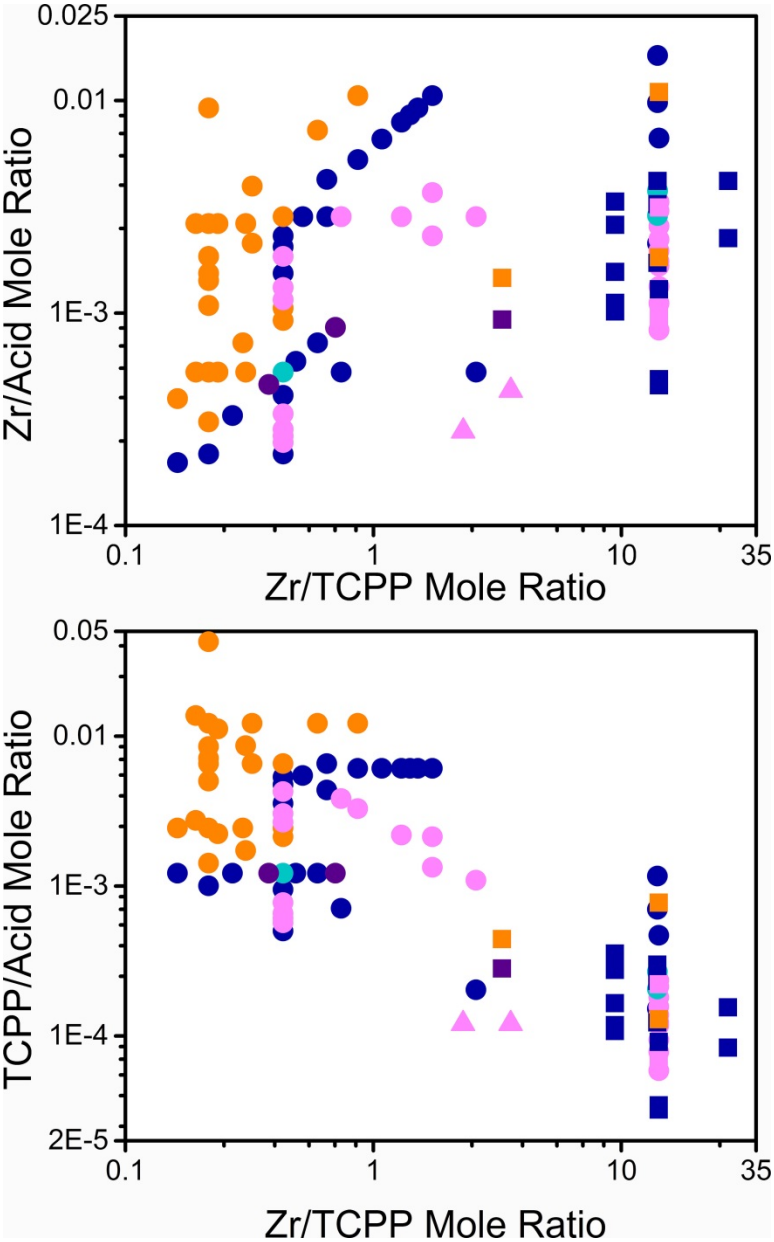

Figure S7 | Results for the 99 reactions heated at 90 °C with $ZrOCl_2 \cdot 8H_2O$ used as the zirconium source. The molar zirconium to porphyrin ratio is plotted along the x-axis while the molar zirconium to acid (top) and porphyrin to acid (bottom) ratios are plotted along the y-axes. Data points indicate the acid used in the reaction and the structure assignment made by the pattern matching MATLAB program (See Figure S6).

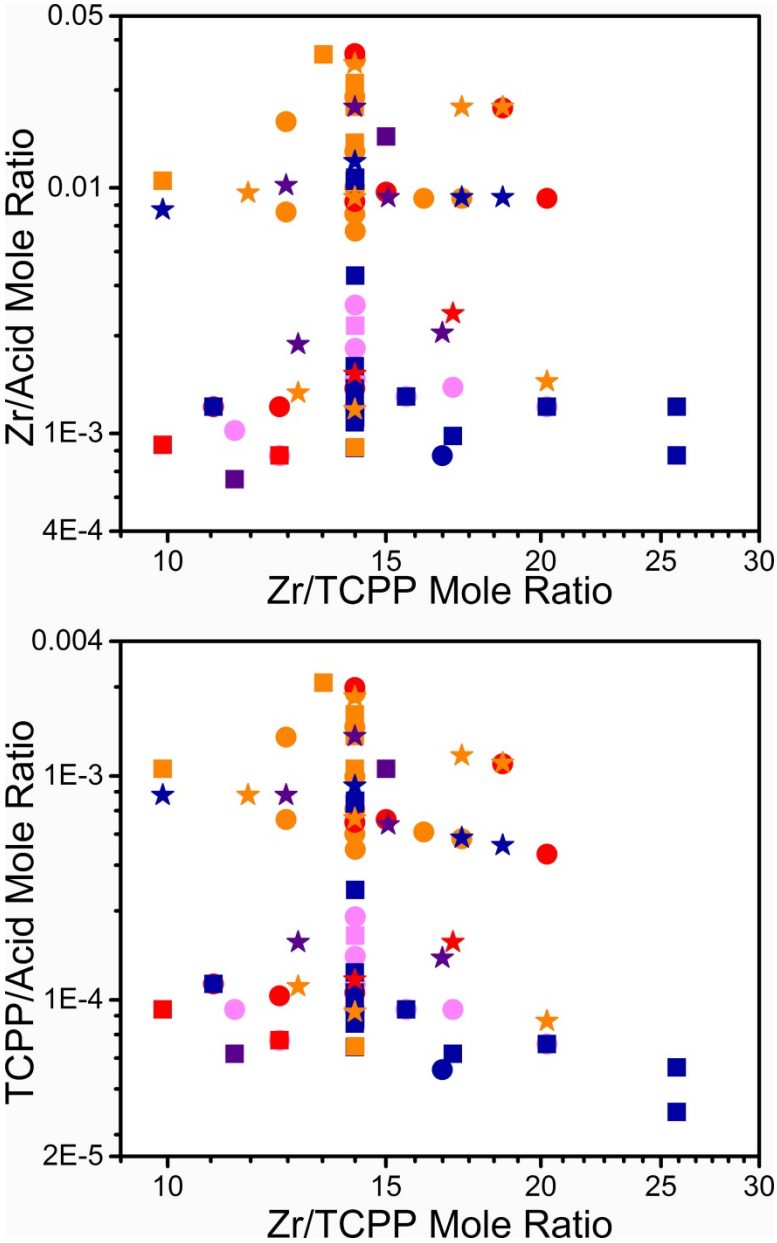

Figure S8 | Results for the 74 reactions heated at 130 °C with $ZrOCl_2 \cdot 8H_2O$ used as the zirconium source. The molar zirconium to porphyrin ratio is plotted along the x-axis while the molar zirconium to acid (top) and porphyrin to acid (bottom) ratios are plotted along the y-axes. Data points indicate the acid used in the reaction and the structure assignment made by the pattern matching MATLAB program (See Figure S6).

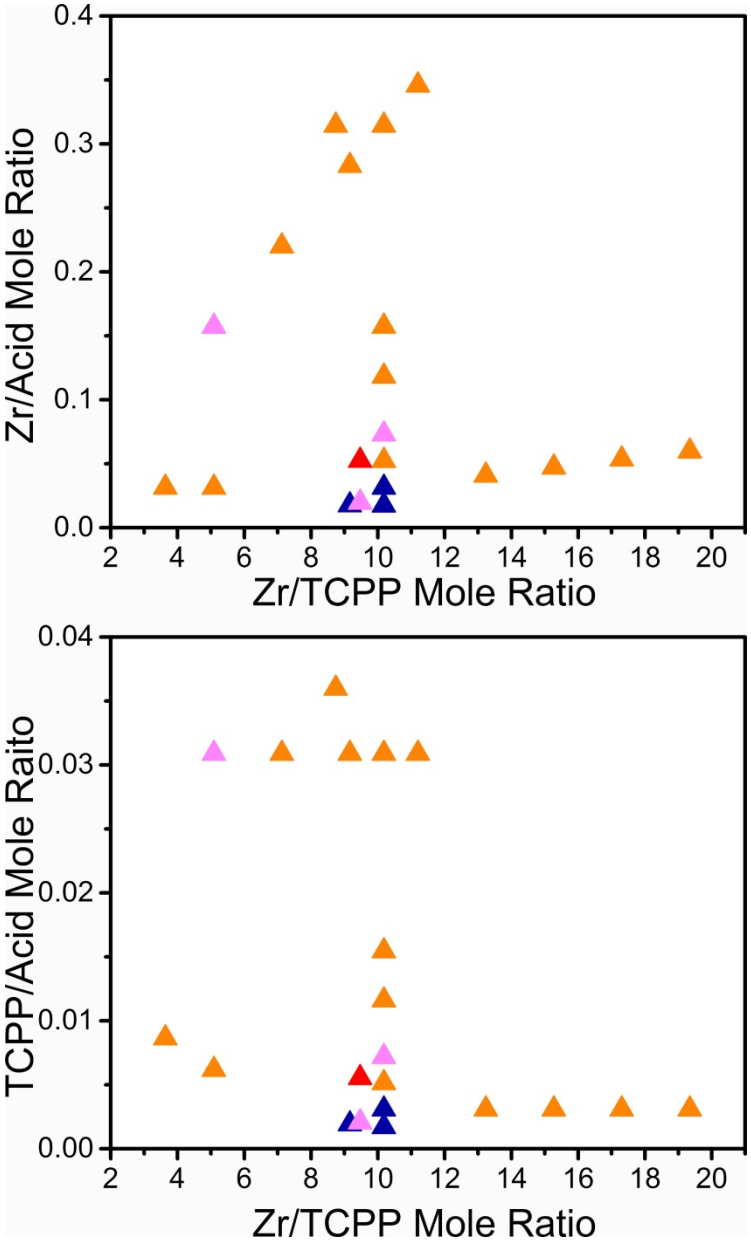

Figure S9 | Results for the 21 reactions heated at 90 °C with $ZrCl_4$ used as the zirconium source. The molar zirconium to porphyrin ratio is plotted along the x-axis while the molar zirconium to acid (top) and porphyrin to acid (bottom) ratios are plotted along the y-axes. Data points indicate the acid used in the reaction and the structure assignment made by the pattern matching MATLAB program (See Figure S6).

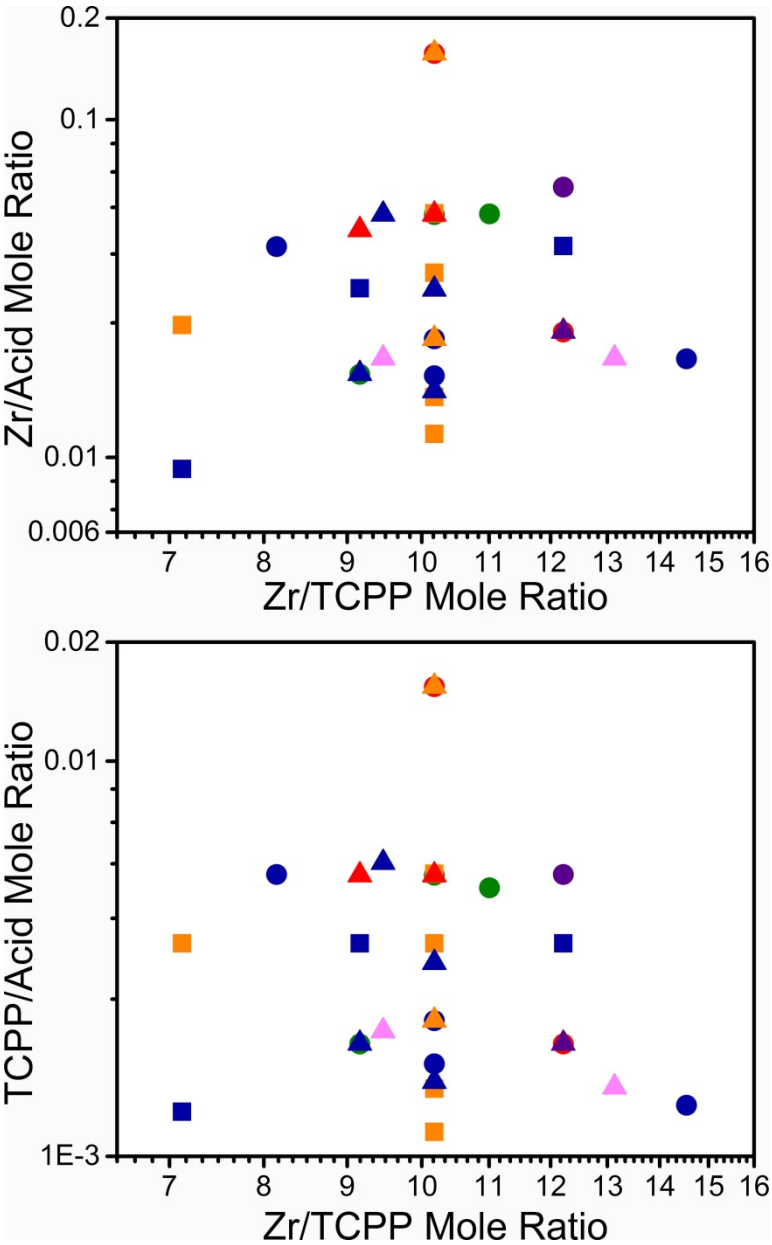

Figure S10 | Results for the 30 reactions heated at 130 °C with $ZrCl_4$ used as the zirconium source. The molar zirconium to porphyrin ratio is plotted along the x-axis while the molar zirconium to acid (top) and porphyrin to acid (bottom) ratios are plotted along the y-axes. Data points indicate the acid used in the reaction and the structure assignment made by the pattern matching MATLAB program (See Figure S6).

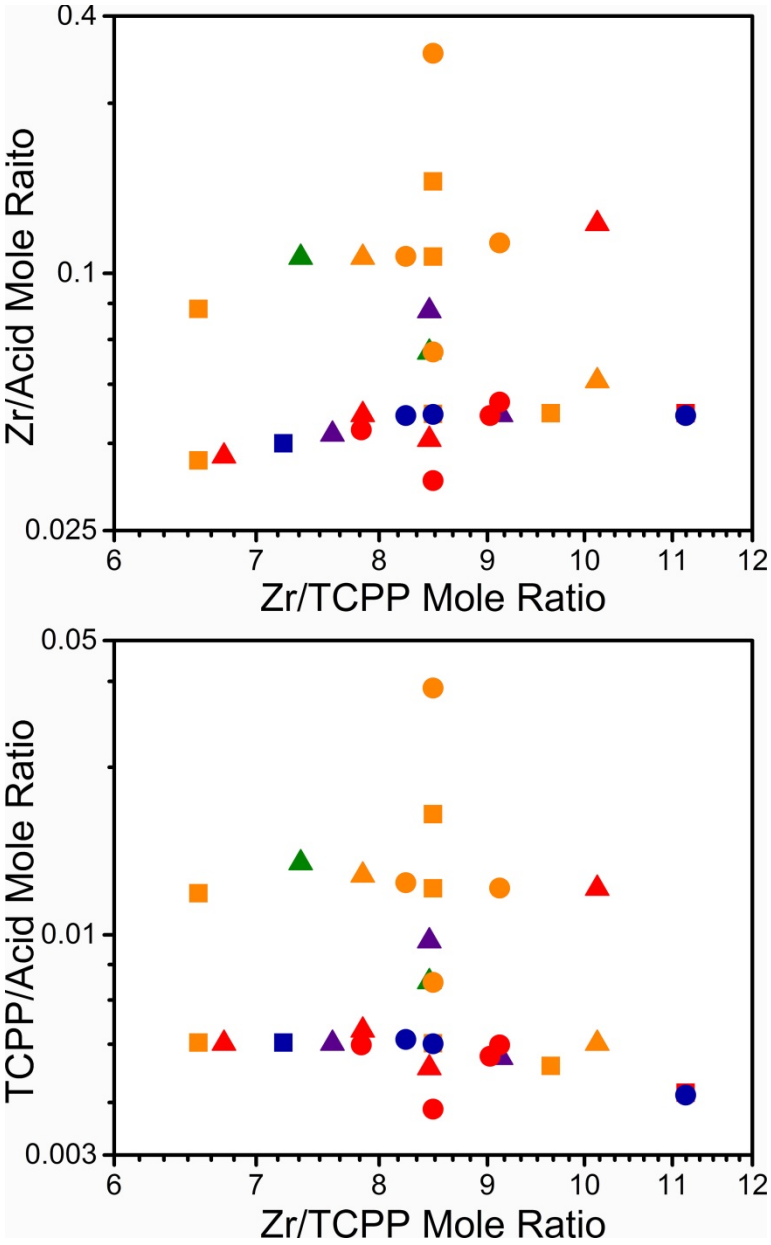

Figure S11 | Results for the 30 reactions heated at 120 °C with $ZrCl_4$ used as the zirconium source. The molar zirconium to porphyrin ratio is plotted along the x-axis while the molar zirconium to acid (top) and porphyrin to acid (bottom) ratios are plotted along the y-axes. Data points indicate the acid used in the reaction and the structure assignment made by the pattern matching MATLAB program (See Figure S6).

Section S2 | Preparative scale nanocrystalline MOF syntheses

MOF-525 (122(20) nm). $ZrOCl_2 \cdot 8H_2O$ (5.2 mg, 0.0016 mmol) and tetrakis(4-carboxyphenyl)-porphyrin (9.8 mg, 0.012 mmol) were ultrasonically dissolved in DMF (3 mL) in a 22 mL borosilicate vial with a Teflon-lined cap. Acetic acid (0.2 ml, 3.5 mmol) was added, and the ensuing solution was heated at 90 °C for 18 hours to afford pink cubic nanocrystals and a dark purple mother liquor. The nanocrystals were collected by centrifugation (15000 rpm, 5 min) followed by solvent exchange with DMF (3 × 1 mL) and then acetone (3 × 1 mL). The material was then activated for 12 hours at 150 °C under reduced pressure to yield MOF-525 (6.6 mg, 61%).

MOF-525 (256(39) nm). $ZrOCl_2 \cdot 8H_2O$ (5.2 mg, 0.0016 mmol) and tetrakis(4-carboxyphenyl)-porphyrin (9.8 mg, 0.012 mmol) were ultrasonically dissolved in DMF (3 mL) in a 22 mL borosilicate vial with a Teflon-lined cap. Acetic acid (0.3 ml, 5.2 mmol) was added, and the ensuing solution was heated at 90 °C for 18 hours to afford pink cubic nanocrystals and a dark purple mother liquor. The nanocrystals were collected by centrifugation (15000 rpm, 5 min) followed by solvent exchange with DMF (3 × 1 mL) and then acetone (3 × 1 mL). The material was then activated for 12 hours at 150 °C under reduced pressure to yield MOF-525 (7.1 mg, 66%).

MOF-525 (341(62) nm). $ZrOCl_2 \cdot 8H_2O$ (5.2 mg, 0.0016 mmol) and tetrakis(4-carboxyphenyl)-porphyrin (9.8 mg, 0.012 mmol) were ultrasonically dissolved in DMF (3 mL) in a 22 mL borosilicate vial with a Teflon-lined cap. Acetic acid (0.35 ml, 6.1 mmol) was added, and the ensuing solution was heated at 90 °C for 18 hours to afford pink cubic nanocrystals and a dark purple mother liquor. The nanocrystals were collected by centrifugation (15000 rpm, 5 min) followed by solvent exchange with DMF (3 × 1 mL) and then acetone (3 × 1 mL). The material was then activated for 12 hours at 150 °C under reduced pressure to yield MOF-525 (5.2 mg, 48%).

MOF-545 (117(22) × 34(7) nm). $ZrOCl_2 \cdot 8H_2O$ (37.5 mg, 0.116 mmol) and tetrakis(4-carboxyphenyl)-porphyrin (6.5 mg, 0.0082 mmol) were ultrasonically dissolved in DMF (16.25 mL) in a 22 mL borosilicate vial with a Teflon-lined cap. Dichloroacetic acid (0.25 mL, 3.0 mmol) was added, and the ensuing solution was heated at 130 °C for 18 hours to afford dark purple rod-shaped nanocrystals and a yellow mother liquor. The nanocrystals were collected by centrifugation (15000 rpm, 5 min) followed by solvent exchange with DMF (3 × 1 mL) and then acetone (3 × 1 mL). The material was then activated for 12 hours at 150 °C under reduced pressure to give MOF-545 (10.6 mg, 96%).

MOF-545 (203(35) × 52(11) nm). $ZrOCl_2 \cdot 8H_2O$ (37.5 mg, 0.116 mmol) and tetrakis(4-carboxyphenyl)-porphyrin (6.5 mg, 0.0082 mmol) were ultrasonically dissolved in DMF (16.20 mL) in a 22 mL borosilicate vial with a Teflon-lined cap. Dichloroacetic acid (0.30 mL, 3.6 mmol) was added, and the ensuing solution was heated at 130 °C for 18 hours to afford dark purple rod-shaped nanocrystals and a yellow mother liquor. The nanocrystals were collected by centrifugation (15000 rpm, 5 min) followed by solvent exchange with DMF (3 × 1 mL) and then acetone (3 × 1 mL). The material was then activated for 12 hours at 150 °C under reduced pressure to yield MOF-545 (10.9 mg, 99%).

MOF-545 (501(95) × 122(30) nm). $ZrOCl_2 \cdot 8H_2O$ (37.5 mg, 0.116 mmol) and tetrakis(4-carboxyphenyl)-porphyrin (6.5 mg, 0.0082 mmol) were ultrasonically dissolved in DMF (16.15 mL) in a 22 mL borosilicate vial with a Teflon-lined cap. Dichloroacetic acid (0.35 mL, 4.2 mmol) was added, and the ensuing solution was heated at 130 °C for 18 hours to afford dark purple rod-shaped nanocrystals and a yellow mother liquor. The nanocrystals were collected by centrifugation (15000 rpm, 5 min) followed by solvent exchange with DMF (3 × 1 mL) and then acetone (3 × 1 mL). The material was then activated for 12 hours at 150 °C under reduced pressure to yield MOF-545 (11.0 mg, 100%).

PCN-223 (538(51) × 331(32) nm). $ZrOCl_2 \cdot 8H_2O$ (5.2 mg, 0.016 mmol) and tetrakis(4-carboxyphenyl)-porphyrin (9.8 mg, 0.012 mmol) were ultrasonically dissolved in DMF (3 mL) in a 11 mL borosilicate vial with a Teflon-lined cap. Acetic acid (0.40 mL, 7.0 mmol) was added, and the ensuing solution was heated at 90 °C for 18 hours to afford pink ellipsoidal nanocrystals and a dark purple mother liquor. The nanocrystals were collected by centrifugation (15000 rpm, 5 min) followed by solvent exchange with DMF (3 × 1 mL) and then acetone (3 × 1 mL). The material was then activated for 12 hours at 150 °C under reduced pressure to yield PCN-223 (8.3 mg, 69%).

PCN-223 (679(159) × 383(74) nm). $ZrOCl_2 \cdot 8H_2O$ (5.2 mg, 0.016 mmol) and tetrakis(4-carboxyphenyl)-porphyrin (9.8 mg, 0.012 mmol) were ultrasonically dissolved in DMF (3 mL) in a 11 mL borosilicate vial with a Teflon-lined cap. Acetic acid (0.55 mL, 9.6 mmol) was added, and the ensuing solution was heated at 90 °C for 18 hours to afford pink ellipsoidal nanocrystals and a dark purple mother liquor. The nanocrystals were collected by centrifugation (15000 rpm, 5 min) followed by solvent exchange with DMF (3 × 1 mL) and then acetone (3 × 1 mL). The material was then activated for 12 hours at 150 °C under reduced pressure to yield PCN-223 (8.0 mg, 66%).

PCN-223 (804(133) × 400(59) nm). $ZrOCl_2 \cdot 8H_2O$ (5.2 mg, 0.016 mmol) and tetrakis(4-carboxyphenyl)-porphyrin (9.8 mg, 0.012 mmol) were ultrasonically dissolved in DMF (3 mL) in a 11 mL borosilicate vial with a Teflon-lined cap. Acetic acid (0.60 mL, 10.5 mmol) was added, and the ensuing solution was heated at 90 °C for 18 hours to afford pink ellipsoidal nanocrystals and a dark purple mother liquor. The nanocrystals were collected by centrifugation (15000 rpm, 5 min) followed by solvent exchange with DMF (3 × 1 mL) and then acetone (3 × 1 mL). The material was then activated for 12 hours at 150 °C under reduced pressure to yield PCN-223 (5.8 mg, 48%).

Section S3 | Theoretical internal and external surface area

The accessible internal surface area was calculated [10] from published crystal structures[Error! Bookmark not defined.,Error! Bookmark not defined.] and found to be 3043.45 m^2/g, 3297.46 m^2/g, and 2763.69 m^2/g for MOF-525, MOF-545, and PCN-223, respectively. The calculated accessible surface area is higher than experimental values reported for each structure and could suggest incomplete activation or the presence of impurities. The internal surface area was converted from m^2/g to nm^2/particle to allow for a direct comparison to the calculated external surface area. The external surface area of each MOF was calculated assuming a perfect geometry and uniform particle size. The actual external surface area is predicted to be lower than the value calculated due to defects and voids on the surface of the particles. The ratio of internal to external surface area increases with increasing particle size.

The external surface area for MOF-525 was estimated using a cube with dimensions a x a x a and the equation $SA = 6a^2$. The external surface area for MOF-545 was estimated using a rectangular prism of dimensions a x a x b and the equation $SA = 4ba + 2a^2$. The external surface area for PCN-223 was estimated using an ellipsoid with dimensions 2a x 2b x 2b and the equation $SA = 4\pi[(2(ab)^{1.6} + (b^2)^{1.6})/3]^{1/1.6}$.

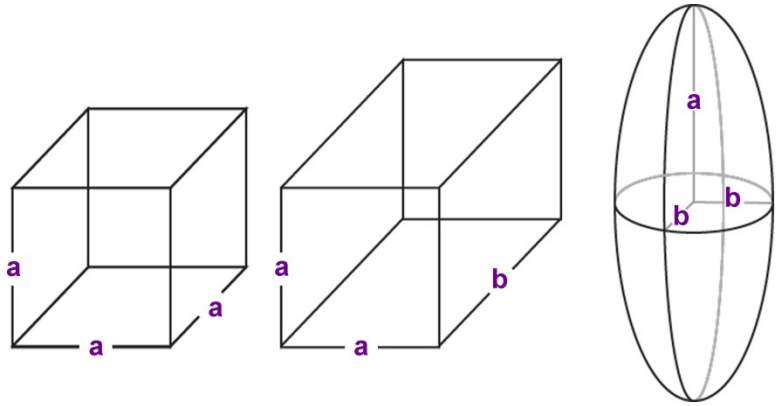

MOF	Size (nm)	External Surface Area/Particle (nm^2/particle)	Theoretical Internal Surface Area/Particle (nm^2/particle)	Ratio of External to Internal Surface Area
MOF-525	122(20)	89,304(20,704)	3,283,657	36.8
MOF-525	256(39)	393,216(91,163)	30,338,790	77.2
MOF-525	341(62)	697,686(161,750)	71,703,688	103
MOF-545	117(22) x 34(7)	18,224(4,488)	241,049	13.4
MOF-545	203(35) x 52(11)	47,639(11636)	978,281	20.4
MOF-545	502(95) x 122(30)	274,744(76,716)	13,316,318	48.4
PCN-223	535(51) x 331(32)	491,912(55,673)	66,987,654	136
PCN-223	679(159) x 383(74)	710,651(182,673)	113,144,160	159
PCN-223	804(133) x 400(59)	862,070(166,132)	146,130,494	170

Table S6 | Reaction conditions carried out using high-throughput synthesis. The robot dispensed solutions to a maximum of 96 reactions in each run. In total, 1036 reactions were set up, and of those reactions, 1027 were unique sets of conditions. Color-coding of the cells is used to indicate which zirconium or acid source was used. Increments given correspond to the reactant cell that displays a range of amounts.

Color Legend

Reactants	
$ZrOCl_2 \cdot 8H_2O$	Blue
$ZrCl_4$	Red
Dichloroacetic acid	Purple
Acetic acid	Green
Benzoic acid	Teal
Formic acid	Orange

Run 1					
130 °C, 72 hrs.	DMF	Reactant Amount (millimoles)			
Reaction Vials	Volume (mL)	TCPP	Zirconium	Acid	Increment
1-10	1.1	0.000548	0.00776	1.33-0.133	0.133
11	1.1	0.000581	0.00776	0.933	
12-16	1.1	0.000515-0.000384	0.00776	0.933	0.0000329
17	1.1	0.000581	0.00776	0.4	
18-21	1.1	0.000515-0.000416	0.00776	0.4	0.0000329
22	1.1	0.000548	0.00822	0.733	
23-27	1.1	0.000548	0.00729-0.00543	0.733	0.000465
28	1.1	0.000548	0.00822	0.4	
29-32	1.1	0.000548	0.00729-0.00590	0.4	0.000465
33-42	1.1	0.000547	0.00776	1.21-0.121	0.121
43	1.1	0.000581	0.00776	0.942	
44-48	1.1	0.000515-0.000384	0.00776	0.942	0.0000329
49	1.1	0.000581	0.00776	0.404	
50-53	1.1	0.000515-0.000416	0.00776	0.404	0.0000329
54	1.1	0.000548	0.00822	0.942	
55-59	1.1	0.000548	0.00729-0.00543	0.942	0.000465
60	1.1	0.000548	0.00822	0.404	
61-64	1.1	0.000548	0.00729-0.00590	0.404	0.000465
65-74	1.1	0.000548	0.00776	0.8	0.080
75	1.1	0.000581	0.00776	0.56	
76-80	1.1	0.000515-0.000384	0.00776	0.56	0.0000329
81	1.1	0.000581	0.00776	0.245	
82-85	1.1	0.000515-0.000416	0.00776	0.245	0.0000329
86	1.1	0.000548	0.000822	0.56	
87-91	1.1	0.000548	0.00729-0.00543	0.56	0.000465
92	1.1	0.000548	0.00822	0.245	
93-96	1.1	0.000548	0.00729-0.00590	0.245	0.000465

Run 2					
130 °C, 72 hrs.	DMF	Reactant Amount (millimoles)			
Reaction Vials	Volume (mL)	TCPP	Zirconium	Acid	Increment
1-10	1	0.00632	0.0644	4.093-0.409	0.409
11-12	1	0.00727-0.0068	0.0644	3.274	0.000474
13-16	1	0.00585-0.00443	0.0644	3.274	0.000474
17-18	1	0.007271-0.0068	0.0644	1.288	0.000474
19-21	1	0.00585-0.0049	0.0644	1.228	0.000474
22-23	1	0.00632	0.0772-0.0708	3.274	0.00644
24-27	1	0.00632	0.0579-0.0386	3.274	0.00644
28-29	1	0.00632	0.0772-0.0708	1.228	0.00644
30-32	1	0.00632	0.0579-0.0451	1.228	0.00644
33-42	1	0.00632	0.0644	4.098-0.410	0.41
43-44	1	0.00727-0.0068	0.0644	3.287	0.000474
45-48	1	0.00585-0.00443	0.0644	3.287	0.000474
49-50	1	0.00727-0.0068	0.0644	1.224	0.000474
51-53	1	0.00585-0.0049	0.0644	1.224	0.000474
54-55	1	0.00632	0.0772-0.0708	3.287	0.00644
56-59	1	0.00632	0.0579-0.0386	3.287	0.00644
60-61	1	0.00632	0.0772-0.0708	1.224	0.00644
62-64	1	0.00632	0.0579-0.0451	1.224	0.00644
65-74	1	0.00632	0.0644	6.095-0.609	0.6095
75-76	1	0.00727-0.0068	0.0644	4.877	0.000474
77-80	1	0.00584-0.00443	0.0644	4.877	0.000474
81-82	1	0.00727-0.0068	0.0644	1.829	0.000474
83-85	1	0.00585-0.0049	0.0644	1.829	0.000474
86-87	1	0.00632	0.0772-0.0708	4.877	0.00644
88-91	1	0.00632	0.0579-0.0386	4.877	0.00644
92-93	1	0.00632	0.0772-0.0708	1.829	0.00644
94-96	1	0.00632	0.0579-0.0451	1.829	0.00644

Run 3					
90 °C, 72 hrs.	DMF	Reactant Amount (millimoles)			
Reaction Vials	Volume (mL)	TCPP	Zirconium	Acid	Increment
1-10	1	0.00632	0.0644	4.093-0.409	0.409
11-12	1	0.00727-0.0068	0.0644	3.274	0.000474
13-16	1	0.00585-0.00443	0.0644	3.274	0.000474
17-18	1	0.007271-0.0068	0.0644	1.288	0.000474
19-21	1	0.00585-0.0049	0.0644	1.228	0.000474
22-23	1	0.00632	0.0772-0.0708	3.274	0.00644
24-27	1	0.00632	0.0579-0.0386	3.274	0.00644
28-29	1	0.00632	0.0772-0.0708	1.228	0.00644
30-32	1	0.00632	0.0579-0.0451	1.228	0.00644

Run 4					
120 °C, 18 hrs.	DEF	Reactant Amount (millimoles)			
Reaction Vials	Volume (mL)	TCPP	Zirconium	Acid	Increment
1-10	1	0.00632	0.0534	1.636-0.164	0.164
11-12	1	0.00727-0.00680	0.0534	1.145	0.000474
13-16	1	0.00585-0.00443	0.0534	1.145	0.000474
17-18	1	0.00727-0.00680	0.0534	0.491	0.000474
19-21	1	0.00585-0.0049	0.00534	0.491	0.000474
22-23	1	0.00632	0.0641-0.0588	1.145	0.00534
24-27	1	0.00632	0.0481-0.0321	1.145	0.00534
28-29	1	0.00632	0.0641-0.0588	0.491	0.00534
30-32	1	0.00632	0.0481-0.0374	0.491	0.00534
33-42	1	0.00632	0.0536	1.64-0.164	0.164
43-44	1	0.0067-0.00651	0.0536	1.154	0.00019
45-48	1	0.00594-0.00481	0.0536	1.154	0.00038
49-50	1	0.0067-0.00651	0.0536	0.49	0.00019
51-53	1	0.00594-0.0518	0.0536	0.49	0.00379
54-55	1	0.00632	0.0577-0.0557	1.154	0.002011
56-59	1	0.00632	0.0496-0.0375	1.154	0.004023
60-61	1	0.00632	0.0577-0.0557	0.49	0.002011
62-64	1	0.000632	0.0496-0.0416	0.49	0.004023
65-74	1	0.00632	0.0536	1.635-0.164	0.164
75-76	1	0.0067-0.00651	0.0536	1.14	0.00019
77-80	1	0.00594-0.00481	0.0536	1.14	0.00038
81-82	1	0.0067-0.00651	0.0536	0.504	0.00019
83-85	1	0.00594-0.00518	0.0536	0.504	0.00038
86-87	1	0.00632	0.0577-0.0557	1.14	0.002011
88-91	1	0.00632	0.0496-0.0375	1.14	0.004023
92-93	1	0.00632	0.0577-0.0557	0.504	0.002011
94-96	1	0.00632	0.0496-0.0416	0.504	0.004023

Run 5					
130 °C, 72 hrs.	DMF	Reactant Amount (millimoles)			
Reaction Vials	Volume (mL)	TCPP	Zirconium	Acid	Increment
1-4	1	0.000457	0.00646	10.337-7.951	0.795
5-10	1	0.000475	0.00646	7.421-3.446	0.795
11-12	1	0.000594-0.000525	0.00646	7.951	0.0000685
13-16	1	0.000388-0.000183	0.00646	7.951	0.0000685
17-18	1	0.000594-0.000525	0.00646	5.036	0.0000685
19-21	1	0.000388-0.000251	0.00646	5.036	0.0000685
22-23	1	0.000457	0.00776-0.00711	7.951	0.000646
24-27	1	0.000457	0.00582-0.00388	7.951	0.000646
28-29	1	0.000457	0.00776-0.00711	5.036	0.000646
30-32	1	0.000457	0.00582-0.00453	5.036	0.000646
33-36	1	0.000457	0.00646	10.347-7.960	0.796
37-42	1	0.000457	0.00646	7.428-3.449	0.796
43-44	1	0.000594-0.000525	0.00646	7.956	0.0000685
45-48	1	0.000388-0.000183	0.00646	7.956	0.0000685
49-50	1	0.000594-0.000525	0.00646	5.036	0.0000685
51-53	1	0.000388-0.000251	0.00646	5.036	0.0000685
54-55	1	0.000457	0.00776-0.00711	7.956	0.000646
56-59	1	0.000457	0.00582-0.00388	7.956	0.000646
60-61	1	0.000457	0.00776-0.00711	5.036	0.000646
62-64	1	0.000457	0.00582-0.00453	5.036	0.000646
65-68	1	0.000457	0.00646	5.168-3.976	0.398
69-74	1	0.000457	0.00646	3.711-1.723	0.398
75-76	1	0.000594-0.000525	0.00646	3.976	0.0000685
77-80	1	0.000388-0.000183	0.00646	3.976	0.0000685
81-82	1	0.000594-0.000525	0.00646	2.521	0.0000685
83-85	1	0.000388-0.000251	0.00646	2.521	0.0000685
86-87	1	0.000457	0.00776-0.00711	3.976	0.000646
88-91	1	0.000457	0.00582-0.00388	3.976	0.000646
92-93	1	0.000457	0.00776-0.00711	2.521	0.000646
94-96	1	0.000457	0.00582-0.00453	2.521	0.000646

Run 6						
90 °C, 18 hrs.	DMF		Reactant Amount (mmol)			
Reaction Vial	Volume (mL)	Increment (mL)	TCPP	Zirconium	Acid	Increment
1-16	0.9-1.65	0.05	0.0149	0.00323	0.00175-0.0149	0.000874
17-32	1.0-1.375	0.025	0.0149	0.000807-0.00686	0.00612	0.000403
33-48	0.9-1.275	0.025	0.00870-0.0180	0.00323	0.00612	0.000622
49-64	0.6-1.35	0.05	0.000746	0.00323	0.00175-0.0149	0.000874
65-80	0.7-1.075	0.025	0.00746	0.000807-0.00686	0.00612	0.000403
81-92	0.6-0.875	0.025	0.00124-0.00808	0.00323	0.00612	0.000622

Run 7						
90 °C, 18 hrs.	DMF		Reactant Amount (mmol)			
Reaction Vial	Volume (mL)	Increment (mL)	TCPP	Zirconium	Acid	Increment
1-16	0.81-0.885	0.005	0.00746	0.00161	0.175-1.486	0.0874
17-32	0.785-1.16	0.025	0.00746	0.000807-0.000686	0.612	0.000403
33-48	0.585-0.96	0.025	0.00435-0.00902	0.00161	0.612	0.000311
49-64	1.02-1.17	0.01	0.00746	0.00323	0.350-2.972	0.175
65-70	0.965-1.215	0.05	0.00746	0.00161-0.00565	1.137	0.000807
71-80	0.635-0.86	0.025	0.00373	0.00323-0.00686	0.612	0.000403
81-92	0.565-1.115	0.05	0.00124-0.00808	0.00323	1.137	0.000622
93-96	0.8-0.86	0.02	0.00373	0.00645	1.749-2.798	0.35

Run 8						
90 °C, 72 hrs.	DMF		Reactant Amount (mmol)			
Reaction Vial	Volume (mL)	Increment (mL)	TCPP	Zirconium	Acid	Increment
1-8	0.55-0.9	0.05	0.00506	0.0257-0.0618	0.164	0.00515
9-16	0.925-1.1	0.025	0.00253	0.0335-0.0515	0.819	0.00257
17-19	0.8-0.866	0.33	0.00506	0.0515	0.164-0.272	0.054
20-22	0.9-0.966	0.33	0.00506	0.0515	0.328-0.436	0.054
23-25	0.5-0.53	0.015	0.00253	0.0257	0.246-0.295	0.0246
26-28	0.55-0.58	0.015	0.00253	0.0257	0.328-0.377	0.0246
29-31	0.6-0.63	0.0015	0.00253	0.0257	0.409-0.459	0.0246
32	0.65		0.00253	0.0257	0.491	
33-35	0.7-0.766	0.033	0.00253-0.00420	0.0515	0.164	0.000835
36-38	0.8-0.866	0.033	0.00506-0.00673	0.0515	0.164	0.000835
39-41	0.9-0.93	0.015	0.00379-0.00455	0.0257	0.819	0.000379
42-44	0.95-0.98	0.015	0.00506-0.00582	0.0257	0.819	0.000379
45-47	1-1.03	0.015	0.00632-0.00708	0.0257	0.819	0.000379
48	1.05		0.00759	0.0257	0.819	
49-59	0.65-0.9	0.025	0.000632	0.000970-0.00259	5.241	0.000162
60-61	0.463-0.487	0.012	0.000316	0.00138-0.00153	2.62	0.0000776
63-64	0.5-0.513	0.013	0.000316	0.00162-0.00170	2.62	0.0000840
65-72	0.8-0.975	0.025	0.000632-0.00119	0.00194	5.241	0.0000790
73-74	0.5-0.513	0.013	0.000632-0.000673	0.00097	2.62	0.0000411
75-76	0.525-0.537	0.012	0.000711-0.000749	0.00097	2.62	0.0000379
77-78	0.55-0.563	0.013	0.000790-0.000831	0.00097	2.62	0.0000411
79-80	0.58-0.6	0.02	0.000885-0.000948	0.00097	2.61	0.0000632
81-88	0.7-0.875	0.025	0.000632	0.00194	3.494-6.551	0.437
89-90	0.45-0.463	0.013	0.000316	0.00097	3.494-3.721	0.227
91-92	0.475-0.487	0.012	0.000316	0.00097	3.93-4.140	0.21
93-94	0.5-0.513	0.013	0.000316	0.00097	4.367-4.594	0.227
95-96	0.525-0.55	0.025	0.000316	0.00097	4.804-5.241	0.437

Run 9					
90 °C, 18 hrs.	DMF	Reactant Amount (millimoles)			
Reaction Vials	Volume (mL)	TCPP	Zirconium	Acid	Increment
1-48	1.6	0.000821	0.0116	0.349-16.770	0.349
49-96	1.6	0.000821	0.0116	0.530-25.444	0.53

Run 10					
130 °C, 18 hrs.	DMF	Reactant Amount (millimoles)			
Reaction Vials	Volume (mL)	TCPP	Zirconium	Acid	Increment
1-48	1.6	0.000821	0.0116	0.349-16.770	0.349
49-96	1.6	0.000821	0.0116	0.530-25.444	0.53

Run 11					
90 °C, 18 hrs.	DMF	Reactant Amount (millimoles)			
Reaction Vials	Volume (mL)	TCPP	Zirconium	Acid	Increment
1-24	0.57	0.000277	0.00388	3.727-0.0793	0.159
25-48	0.57	0.000277	0.00388	6.228-0.133	0.265
49-60	0.57	0.000144	0.00388	3.578-0.663	0.265
61-72	0.57	0.000329	0.0031	3.578-0.663	0.265
73-84	0.57	0.000411	0.00136	3.578-0.663	0.265
85-96	0.57	0.0000822	0.00485	3.578-0.663	0.265

Run 12						
90 °C, 18hrs	DMF		Reactant Amount (millimoles)			
Reaction Vial	Volume (mL)	Increment (mL)	TCPP	Zirconium	Acid	Increment
1-16	0.770-0.920	0.1	0.00310	0.00403	0.349-2.970	0.175
17-32	0.770-0.920	0.1	0.00316	0.00403	0.349-2.970	0.175
33-48	0.770-0.920	0.1	0.00349	0.00403	0.349-2.970	0.175

References

(1) L. J. Twyman, A. Ellis and P. J. Gittins, *Macromolecules*, 2011**, 44**, 6365.
(2) W. Morris, B. Volosskiy, S. Demir, F. Gándara, P. L. McGrier, H. Furukawa, D. Cascio, J. F. Stoddart and O. M. Yaghi, *Inorg. Chem.*, 2012**, 51**, 6443.
(3) D. Feng, Z.-Y. Gu, Y.-P. Chen, J. Park, Z. Wei, Y. Sun, M. Bosch, S. Yuan and H.-C. Zhou, *J. Am. Chem. Soc.*, 2014, **136**, 17714.
(4) D. Feng, W.-C. Chung, Z. Wei, Z.-Y. Gu, H.-L. Jiang, Y.-P. Chen, D. J. Darensbourg and H.-C. Zhou, *J. Am. Chem. Soc.*, 2013, **135**, 17105.
(5) H.-L. Jiang, D. Feng, K. Wang, Z.-Y. Gu, Z. Wei, Y.-P. Chen, and H.-C. Zhou, *J. Am. Chem. Soc.*, 2013, **135**, 13934.
(6) A. Schaate, P. Roy, A. Godt, J. Lippke, F. Waltz, M. Wiebcke and P. Behrens, *Chem. –Eur. J.*, 2011, **17**, 6643.
(7) H. Wu, Y. S. Chua, V. Krungleviciute, M. Tyagi, P. Chen, T. Yildirim and W. Zhou, *J. Am. Chem. Soc.*, 2013, **135**, 10525.
(8) C. A. Trickett, K. J. Gagnon, S. Lee, F. Gándara, H.-B. Bürgi and O. M. Yaghi, *Angew. Chem. Int. Ed.*, 2015, **54**, 11162.
(9) O. V. Gutov, M. G. Hevia, E. C. Escudero Adán and A. Shafir, *Inorg. Chem.*, 2015, **54**, 8396.
(10) T. Düren, F. Millange, G. Férey, K. S. Walton and R. Q. Snurr, *J. Phys. Chem. C*, 2007, ***111***, 15350.